ing homology (*15*). Second, the alignments are well defined. No gaps are needed to align the eukaryotic and eocytic EF-1α sequences, and no gaps are needed to align the EF-2 and the IF-2 sequences with those EF-1α sequences that contain the four–amino acid segment (except for three amino acids unique to *Methanococcus vannielii*). Third, the sequences encoding EF-1α are not likely to be laterally transferred between organisms. EF-1α is present in all cells and, during protein synthesis, interacts with cellular components encoded by genes dispersed throughout the bacterial genome, including aminoacyl-tRNAs, ribosomal proteins, elongation factor EF-Ts, and 16*S* and 18*S* ribosomal RNAs (*16*).

Other results also support a sister relationship between the eukaryotes and eocytes. For example, the major heat shock protein of *Sulfolobus shibatae* is a molecular chaperone related to a eukaryotic t-complex gene (*17*). Similarly, the eukaryotic ribosomal RNA operons (*18*) are organized like those of *Sulfolobus*, *Desulfurococcus*, *Thermoproteus*, and *Thermococcus*. By contrast, the tRNA-containing ribosomal RNA operons of halobacteria, methanogens, and eubacteria (*19*) share a different pattern.

Although many characters support the eocyte tree (*20*), some do not. First, eubacteria, halobacteria, and eukaryotes share ester-linked fatty acids and functional fatty acid synthetases (*21*). This does not support either the archaebacterial or eocyte tree but does support an alternative topology. Second, halobacteria, methanogens, and eocytes have at least traces of a distinct ether lipid (*22*), which supports the archaebacterial tree and does not support the eocyte tree. If both exceptions were valid, no tree would be acceptable. The exceptions therefore emphasize the need for caution and an appreciation of the chimeric origins (*23*) of some nuclear sequences in an analysis of the phylogenetic relationships of eukaryotes. Reconstruction of the prokaryotic ancestry of eukaryotes requires caution; however, the phylogenetic distribution of the 11–amino acid segment implies that the eocytes are the closest surviving relatives of eukaryotes. This lends support to the proposal (*12*) that the eukaryotes and eocytes comprise a monophyletic superkingdom, the karyotes.

REFERENCES AND NOTES

1. J. Felsenstein, *J. Syst. Zool.* **27**, 401 (1978).
2. J. A. Lake, *Mol. Biol. Evol.* **8**, 378 (1990); D. P. Mindell, in *Phylogenetic Analysis of DNA Sequences*, M. Miyamoto and J. Cracraft, Eds. (Oxford Univ. Press, London, 1991), pp. 119–136.
3. C. Patterson, *Nature* **344**, 199 (1990).
4. J. A. Lake, E. Henderson, M. W. Clark, M. Oakes, *Proc. Natl. Acad. Sci. U.S.A.* **81**, 3786 (1984).
5. F. Jurnak, *Science* **230**, 32 (1985); T. F. M. la Cour, J. Nyborg, S. Thirup, B. F. C. Clark, *EMBO J.* **4**, 2385 (1985).
6. The *E. coli* numbering system was used. Abbreviations for the amino acid residues are: A, Ala; C, Cys; D, Asp; E, Glu; F, Phe; G, Gly; H, His; I, Ile; K, Lys; L, Leu; M, Met; N, Asn; P, Pro; Q, Gln; R, Arg; S, Ser; T, Thr; V, Val; W, Trp; and Y, Tyr.
7. A. T. Matheson, J. Auer, C. Ramirez, A. Boeck, in *The Ribosome: Structure, Function, and Evolution*, W. E. Hill *et al.*, Eds. (American Society for Microbiology Press, Washington, DC, 1990), pp. 617–633.
8. K. O. Stetter *et al.*, *FEMS Microbiol. Rev.* **75**, 117 (1990).
9. Genomic DNA was isolated from cell pastes of *Desulfurococcus, Pyrodictium*, and *Acidianus* by SDS–proteinase-K lysis (*24*). Genomic DNA was further purified by gel electrophoresis in the presence of ethidium bromide. The high molecular weight band was excised from the gel and melted at 70°C, and a small aliquot was amplified by PCR (*25*). Degenerate primers designed from the amino acid alignments of known EF-1α sequences for the $KNMITG_{94}$ and the $QTREH_{118}$ regions were used for the PCR reactions. PCR products were analyzed by electrophoresis. A single band of approximately 120 bp was purified from agarose gels and cloned into the pCR1000 vector (Invitrogen) according to the manufacturer's recommendations. Colonies containing the insert were sequenced by the dideoxy chain termination method with Sequenase (U.S. Biochemical Corp.) as recommended by the manufacturer.
10. H. R. Bourne, D. A. Sanders, F. McCormick, *Nature* **349**, 117 (1991).
11. C. R. Woese, *Microbiol. Rev.* **51**, 221 (1987).
12. J. A. Lake, *Nature* **331**, 184 (1988).
13. W. M. Fitch, *Am. Nat.* **111**, 223 (1977); E. O. Wiley, *Phylogenetics* (Wiley, New York, 1981).
14. M. O. Dayhoff, W. C. Barker, L. T. Hunt, *Methods Enzymol.* **91**, 524 (1983).
15. M. Waterman and M. Eggert, *J. Mol. Biol.* **197**, 723 (1987).
16. W. E. Hill *et al.*, Eds., *The Ribosome: Structure, Function, and Evolution* (American Society for Microbiology Press, Washington, DC, 1990).
17. J. D. Trent, E. Nimmesgern, J. S. Wall, F.-U. Hartl, A. L. Horwich, *Nature* **354**, 490 (1991).
18. S. A. Gerbi, in *Molecular Evolutionary Genetics*, R. J. MacIntyre, Ed. (Plenum, New York, 1985), pp. 419–517.
19. N. Larsen, H. Leffers, J. Kjems, R. A. Garrett, *System. Appl. Microbiol.* **7**, 49 (1986).
20. J. A. Lake, *Trends Biochem. Sci.* **16**, 46 (1991).
21. M. Kamekura and M. Kates, "Lipids of halophilic archaebacteria," in *Halophilic Bacteria*, F. Rodrigues-Valera, Ed. (CRC Press, Boca Raton, FL, 1988), pp. 25–54.
22. V. Lanzotti *et al.*, *Biochim. Biophys. Acta* **1004**, 44 (1989).
23. M. W. Gray, *Trends Genet.* **5**, 294; L. Margulis, *Symbiosis in Cell Evolution* (Freeman, San Francisco, 1981); S. L. Baldauf and J. D. Palmer, *Nature* **344**, 262 (1990).
24. B. G. Herrmann and A. Frischauf, *Methods Enzymol.* **152**, 180 (1987).
25. R. K. Saiki, in *PCR Protocols: A Guide to Methods and Applications*, M. A. Innis, D. H. Gelfand, J. J. Sninsky, T. J. White, Eds. (Academic Press, New York, 1990), pp. 13–20.
26. J. P. Gogarten *et al.*, *Proc. Natl. Acad. Sci. U.S.A.* **86**, 6661 (1989); N. Iwabe *et al.*, *ibid.*, p. 9355.

27. We thank J. Arrington for technical assistance; A. Scheinman, G. Shankweiler, T. Atha, and A. Aguinaldo for discussions, suggestions and advice; and K. Stetter for cells of eocytes, methanogens, and their relatives. Supported by grants from the NSF, NIH, and the Alfred P. Sloan Foundation to J.A.L.

27 February 1992; accepted 7 May 1992

Conformation of the TAR RNA-Arginine Complex by NMR Spectroscopy

Joseph D. Puglisi, Ruoying Tan, Barbara J. Calnan, Alan D. Frankel, James R. Williamson*

The messenger RNAs of human immunodeficiency virus–1 (HIV-1) have an RNA hairpin structure, TAR, at their 5′ ends that contains a six-nucleotide loop and a three-nucleotide bulge. The conformations of TAR RNA and of TAR with an arginine analog specifically bound at the binding site for the viral protein, Tat, were characterized by nuclear magnetic resonance (NMR) spectroscopy. Upon arginine binding, the bulge changes conformation, and essential nucleotides for binding, U23 and A27·U38, form a base-triple interaction that stabilizes arginine hydrogen bonding to G26 and phosphates. Specificity in the arginine-TAR interaction appears to be derived largely from the structure of the RNA.

The diverse structures formed by RNA molecules contribute to their specific recognition by proteins (*1*, *2*). The interaction of the HIV Tat protein with TAR, an RNA hairpin located at the 5′ end of the viral mRNAs, provides a well-characterized system for the study of RNA-protein recognition. The binding of Tat to TAR is essential for Tat to function as a transcriptional activator (*3–6*). The predicted secondary structure of TAR consists of two stem regions separated by three unpaired nucleotides (a bulge) and a loop of six nucleotides (Fig. 1A). Many mutational studies have identified nucleotides in and near the bulge that are important for specific binding of Tat (*4*, *7–10*). The loop region is not involved in Tat binding but is important for activation of transcription (*4–6*, *10*, *11*). Specific binding of Tat to TAR is mediated by a single arginine (*12*) within a nine-residue stretch of basic amino acids, as shown by specific binding of model peptides

J. D. Puglisi and J. R. Williamson, Department of Chemistry, Massachusetts Institute of Technology, Cambridge, MA 02139.
R. Tan, B. J. Calnan, A. D. Frankel, Whitehead Institute for Biomedical Research, 9 Cambridge Center, Cambridge, MA 02142.

*To whom correspondence should be addressed.

in vitro (6, 10, 13) and by transactivation by mutant Tat proteins in vivo (6, 12, 14). Free arginine also binds specifically to TAR, and chemical interference experiments indicate that arginine interacts with TAR in a similar manner, whether as the free amino acid or in the context of the peptide (15). We performed NMR studies on wild-type and mutant TAR RNAs in the presence or absence of argininamide, a tight-binding arginine analog, that reveal structural features of the RNA responsible for specific Tat-TAR recognition.

Detailed NMR structures have been reported for several small RNA molecules (<20 nucleotides) (16), and nucleotide conformation and base stacking have been reported for larger molecules (17). We determined the conformation of TAR RNA (31 nucleotides) (Fig. 1A) by two-dimensional NMR spectroscopy (Figs. 1, B to D, and 2, A and C). The two stem regions form base-paired, A-form helices with standard nucleotide conformations (18–20). U23, the 5′ nucleotide in the bulge, is stacked on A22. The other two nucleotides give internucleotide base-sugar nuclear Overhauser effects (NOEs) consistent with partial stacking, but the conformation of these nucleotides is not well defined by the NMR data (Fig. 2, A and C). We observed NOEs between helical nucleotides C39 and U40, which suggests only a minor distortion in helix conformation opposite the stacked bulge. The stacked structure of the bulge induces bending in the overall helix axis (21), although our NMR data do not provide direct evidence for bending. The six-nucleotide loop is not directly involved in the interaction of Tat with TAR, and we have not characterized the structure of this loop in detail.

Free arginine interacts with TAR in a manner similar to that of arginine in the context of Tat peptides, as shown by competition and chemical interference experiments (15). To characterize specific binding of arginine to TAR, we monitored the chemical shifts of TAR resonances as a function of argininamide concentration (22). Changes of chemical shift of NMR resonances are a sensitive indicator of changes in local environment that result from binding or conformational changes. The addition of argininamide affected the chemical shifts of nucleotides in the region of the bulge but had little or no effect in the stems or loop (Fig. 3). Chemical shift profiles as a function of argininamide concentration indicate that argininamide binding is specific and saturable (23). All three bulge nucleotides exhibited large downfield changes in chemical shift, and A22(H2) proton resonance below the bulge exhibited a 0.4-ppm shift upfield. Helical nucleotides surrounding the bulge and G28(H8) in the upper stem also exhibited shift changes.

The conformational change of the bulge upon argininamide binding involves unstacking of the three bulge nucleotides, coaxial stacking of the two stems, and formation of an additional RNA-RNA interaction (Fig. 2, B and D). In the argininamide complex, bulge nucleotides were not stacked between the two helical stems, consistent with the large downfield chemical shifts of resonances from these nucleotides and with the loss of internucleotide NOEs upon argininamide binding. The NOE data indicated that U23 is positioned near A27 in the major groove of the upper stem. No internucleotide NOEs were observed from C24 and U25, which suggests that these nucleotides are

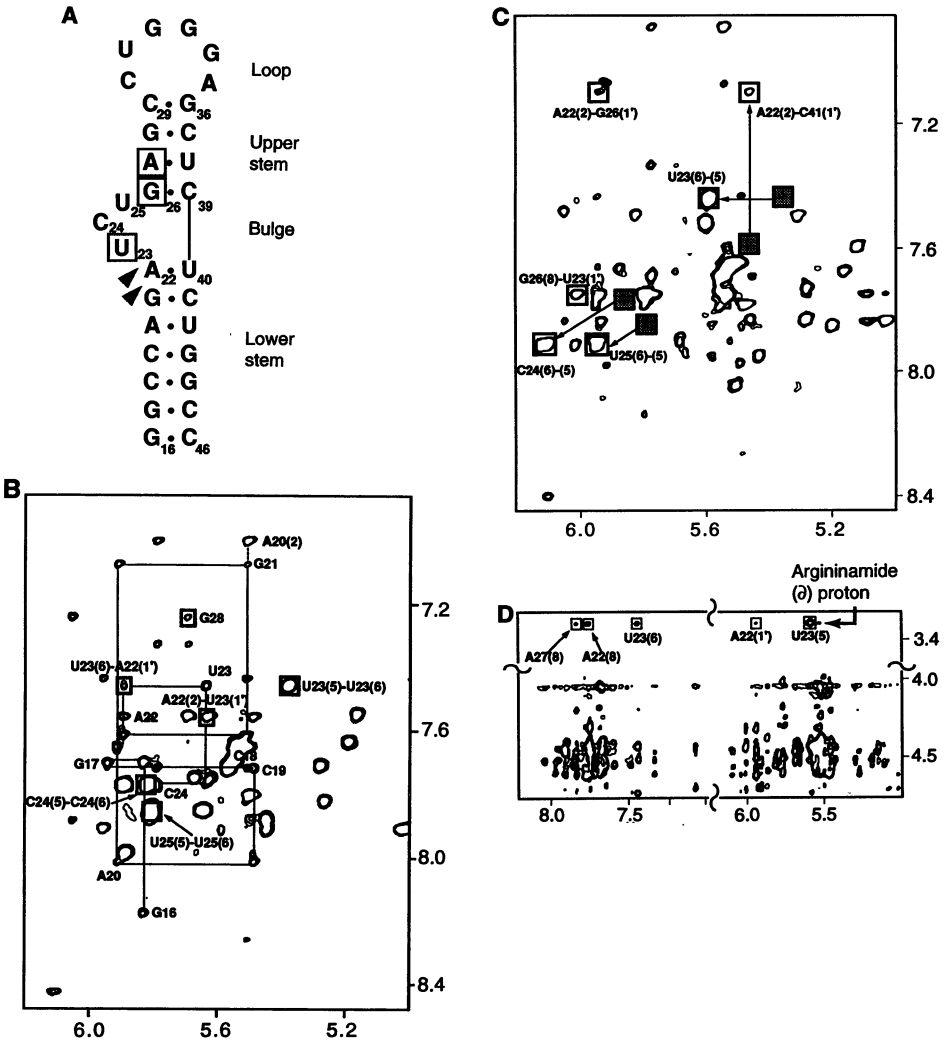

Fig. 1. (**A**) Secondary structure of TAR RNA. Nucleotides important for recognition by Tat are boxed; phosphates whose ethylation interferes with binding of Tat peptides or arginine are marked by arrows. Stem, bulge, and loop regions are labeled. Numbering refers to nucleotides in HIV HXB-2 isolate relative to the cap site; G16, G17, C45, and C46 are not part of HIV TAR and were added to increase the efficiency of in vitro transcription. Different numbering schemes have been used in other studies (usually having values that are one less than shown). (**B**) Two-dimensional NOE (NOESY) spectrum of TAR showing NOEs between aromatic protons (H8/H6/H2) and pyrimidine H5 and ribose H1′. Sequential NOEs between aromatic H8/H6 (n + 1) and sugar H1′ (n) protons from G16 to C24 are indicated by lines connecting cross peaks. Labeled cross peaks correspond to intranucleotide aromatic H1′ NOEs. Cross peaks corresponding to NOEs of structural interest are boxed. (**C**) Same region of the NOESY spectrum as shown in (B) for TAR in the presence of 6 mM argininamide; NOEs that indicate a conformational change are boxed and labeled. Cross peaks for three bulge nucleotides and A22 that shift considerably upon addition of argininamide are highlighted; shaded boxes indicate their position in the absence of argininamide. (**D**) Portion of the NOESY spectrum of TAR + argininamide (6 mM) that shows NOEs between argininamide (δ) protons and protons in TAR. All of the NOESY spectra were obtained with the standard pulse sequence and phase cycling (34). A 400-ms mixing time was used for these experiments. All measurements in (B) to (D) are in parts per million.

not well structured. Although nucleotides C39 and U40 opposite the bulge remained stacked, the stacking of the two base pairs bordering the bulge was probably distorted from standard A-form geometry, as the NOEs between A22 and G26 were much weaker than expected for A-form geometry. All ^{31}P resonances of TAR exhibited normal chemical shifts in both the absence and presence of argininamide. No significant changes in the stem or loop structure were observed.

We observed NOEs (*24*) between argininamide (δ) protons (adjacent to the guanidinium group) and protons on A22, U23, and A27 (Fig. 1D). The most direct interpretation is that the conformational change of TAR results from formation of a single arginine binding pocket, such that these protons are close to the argininamide (δ) protons. Although we could not directly determine the number of arginine binding sites from the NMR data, the data are consistent with a single site.

NMR experiments on a peptide-TAR complex yielded further support for a single arginine binding site. We characterized the structure of TAR bound to an 11–amino acid peptide (YKKKRKKKKKA, where Y is Tyr, K is Lys, R is Arg, and A is Ala) that contains a single arginine and binds specifically to TAR with high affinity (*12*). Peptide binding at 1:1 stoichiometry induced chemical shift changes of TAR resonances similar to those observed on argininamide binding (Fig. 3). The conformation of TAR bound to this peptide was similar to that of TAR bound to argininamide. Intermolecular NOEs were observed between peptide protons and protons on U23 and A22 that indicate specific interaction of the peptide with the bulge region of TAR. The agreement between NMR results obtained with argininamide and those obtained with the peptide is consistent with other biochemical studies (*12*, *15*, *25*).

To further examine specificity of arginine binding, we characterized the structures of two TAR mutants, U23 to C23 or A27·U38 to U27·A38, that showed reduced binding affinity of Tat peptides (*8*). Both mutations disrupted specific argininamide binding (*15*) and the conformational change observed with wild-type TAR. In the absence of argininamide, the bulge nucleotides in each mutant were stacked between the two stems in a conformation similar to that observed in wild-type TAR. Thus, these mutations do not reduce peptide or arginine binding by changing the unbound structure of TAR. The structures of both mutants in the presence of 6 mM argininamide resembled that of wild-type TAR in the absence of argininamide. Bulge nucleotide 23 in both mutants remained stacked on A22 in the presence of argininamide. The presence or absence of conformational changes has been observed by circular dichroism experiments on TAR and TAR mutants (*25*). For both mutants, NOEs were not observed between argininamide and the set of nucleotides for which NOEs were seen in wild-type TAR (*26*). These results further demonstrate the interdependence of specific arginine binding and RNA structure.

Nucleotides in TAR critical for Tat binding and function, such as U23, G26·C39, A27·U38, and phosphates between G21 and A22 (P22) and between A22 and U23 (P23) are distant in the absence of arginine (Fig. 2C) but are in close proximity in the arginine-bound structure (Fig. 2D). A22 and G26 are coaxially stacked in the bound structure. Our NOE data positioned U23 within hydrogen bonding distance of A27·U38 in the major groove, and we propose a base-triple interaction between U23 and A27 (*27*, *28*). The strong NOE from the argininamide (δ) proton to U23(H5) and weaker NOEs to A22 and A27 position argininamide below U23, near G26 (Fig. 2D). A model for the arginine interaction that

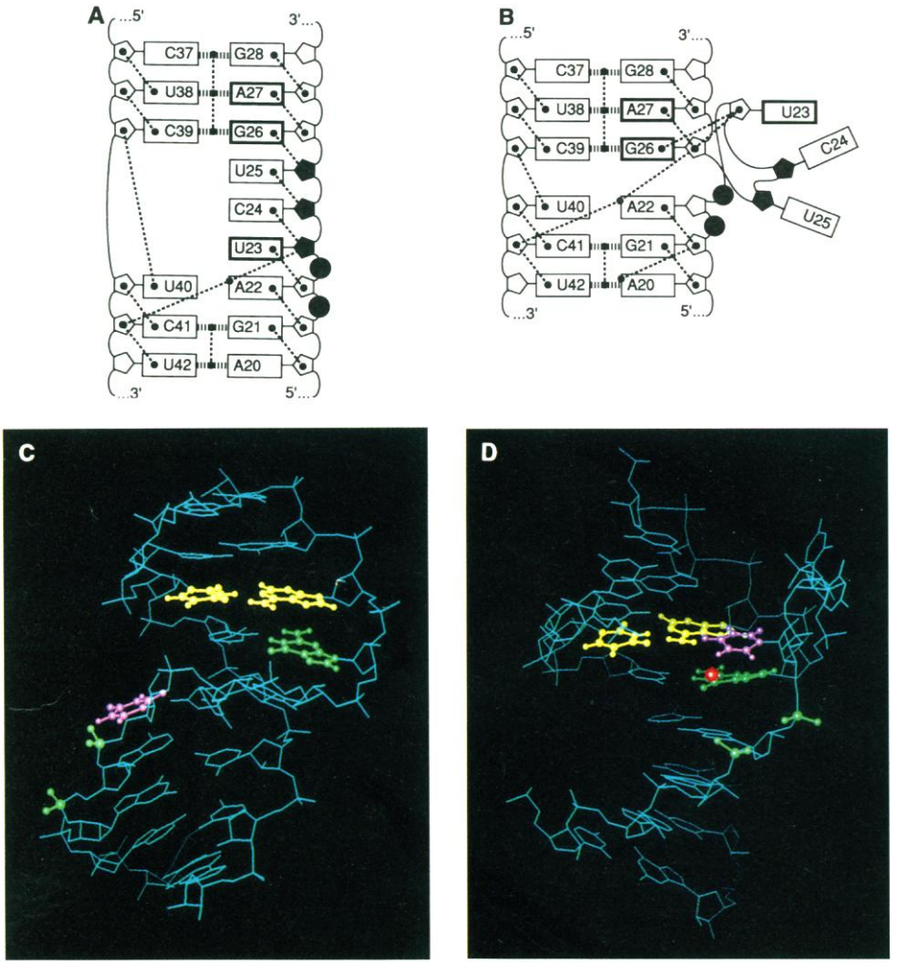

Fig. 2. Schematic structures of the bulge regions of TAR in the absence (**A**) or presence (**B**) of argininamide that summarize the NMR results. Base pair hydrogen bonding derived from imino proton resonances is shown by wide dashed lines between bases. Ribose, base H8/H6, adenine H2, and imino protons are represented by dots within pentagons, on the outside of the bases, on the inside of adenines, or within hydrogen bonds, respectively. Observed internucleotide NOEs are indicated by dashed lines connecting dots; there is no direct correlation between the length of lines indicated and strength of NOEs. Shaded sugars have a $C_{2'}$-*endo* conformation, and all other sugars have primarily a $C_{3'}$-*endo* conformation. Functionally important nucleotides are indicated by bold boxes. Dark circles highlight phosphates whose ethylation interferes with arginine and Tat peptide binding. In (B), no NOEs were observed between C24 and U25, and these nucleotides are represented as disordered. Three-dimensional structures of TAR in the absence (**C**) and presence (**D**) of argininamide were generated as described (*35*). The A27·U38 base pair is yellow, U23 is pink, and G26 and phosphates P22 and P23 are green. In (D), the pseudo-atom corresponding to the arginine (δ) proton is red.

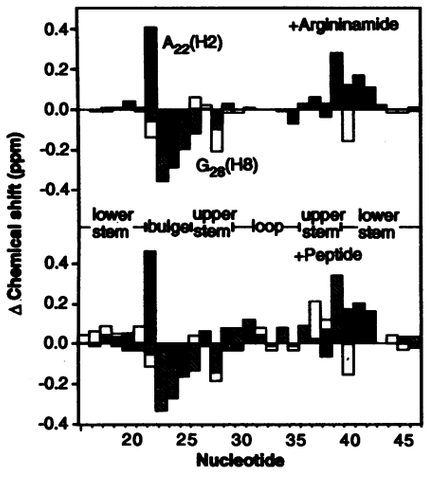

Fig. 3. (**Top**) Plot of changes in chemical shift for TAR H6/H8, H1′, and H2/H5 resonances upon addition of argininamide (3 mM). (**Bottom**) Plot of changes in chemical shift for TAR H6/H8, H1′, and H2/H5 resonances upon formation of 1:1 complex (0.85 mM) with an 11–amino acid peptide that contained a single Arg (R52) (*12*). Chemical shift is measured in parts per million (ppm) from trimethylsilyl propionic acid. Nucleotide position as well as stem, bulge, and loop regions are marked on the abscissa. The H8/H6 proton shift changes are indicated by unfilled bars, H1′ protons by hatched bars, and H2/H5 protons by solid bars. The peptide was synthesized and purified as described (*12*).

is most consistent with our NMR data (Fig. 4) consists of a pair of hydrogen bonds between the guanidinium group and G26 in the major groove and hydrogen bonds to phosphates P22 and P23 that are favorably positioned in the bound structure. The major features of our model are well constrained by the NMR data, and alternate models, in which arginine contacts U23 and A27 directly, do not satisfy the NMR constraints.

Mutational, chemical interference, and functional studies support a role in Tat binding for every functional group involved in the proposed base-triple interaction and formation of the arginine binding site (*4*–*10*, *12*, *13*, *15*, *25*). Mutation of A27·U38 or alkylation of A27(N7) interferes with peptide and arginine binding (*8*, *15*); these modifications disrupt the A27(N6) and N7 groups required for the triple interaction. Similarly, modifications of the U23(O4) (*8*, *9*, *15*) and N3 (*9*) groups also abolished specific binding. The proposed contact of arginine with G26·C39 is supported by the reduced peptide affinity for an A26·U39 mutant (*8*) and by strong interference when G26(N7) is methylated (*13*); the proposed arginine-guanine interaction has been observed in crystal structures of many DNA-protein complexes (*29*). Mutation of the G26·C39 base pair reduces transactivation in vivo (*30*). The interaction of arginine with the phosphate oxygens of P22 and P23 is supported by ethylation interference of peptide and arginine binding (*12*, *15*). The identity of other bulge nucleotides (C24 and U25) is not important for Tat binding (*8*, *9*), which is consistent with a bound structure in which these nucleotides are unstacked in solution and do not interact with arginine or TAR. In addition, a TAR mutant with a bulge of only two uridines binds Tat peptides as well as wild-type TAR (*8*); the base triple and other conformational changes that occur upon arginine binding should be accommodated by a bulge of only two nucleotides.

Our model incorporates features of previous models for specific interaction of Tat and TAR. In the arginine fork model (*12*), arginine is proposed to recognize TAR, at least in part, by forming hydrogen bonds with two phosphates held in a precise orientation by the structure of the bulge. The interaction of arginine with phosphates in our model is stabilized by the base-triple interaction. Another model proposes that the bulge serves to increase accessibility of specific groups in the major groove (*8*). This appears to be critical for the formation of the base-triple interaction between U23 and A27·U38 and for direct arginine binding to G26. An alternate RNA tertiary interaction involving U23 and G26 has also been proposed (*9*). Our model assigns a functional role in the Tat-TAR interaction to each important chemical group determined by chemical and mutational studies.

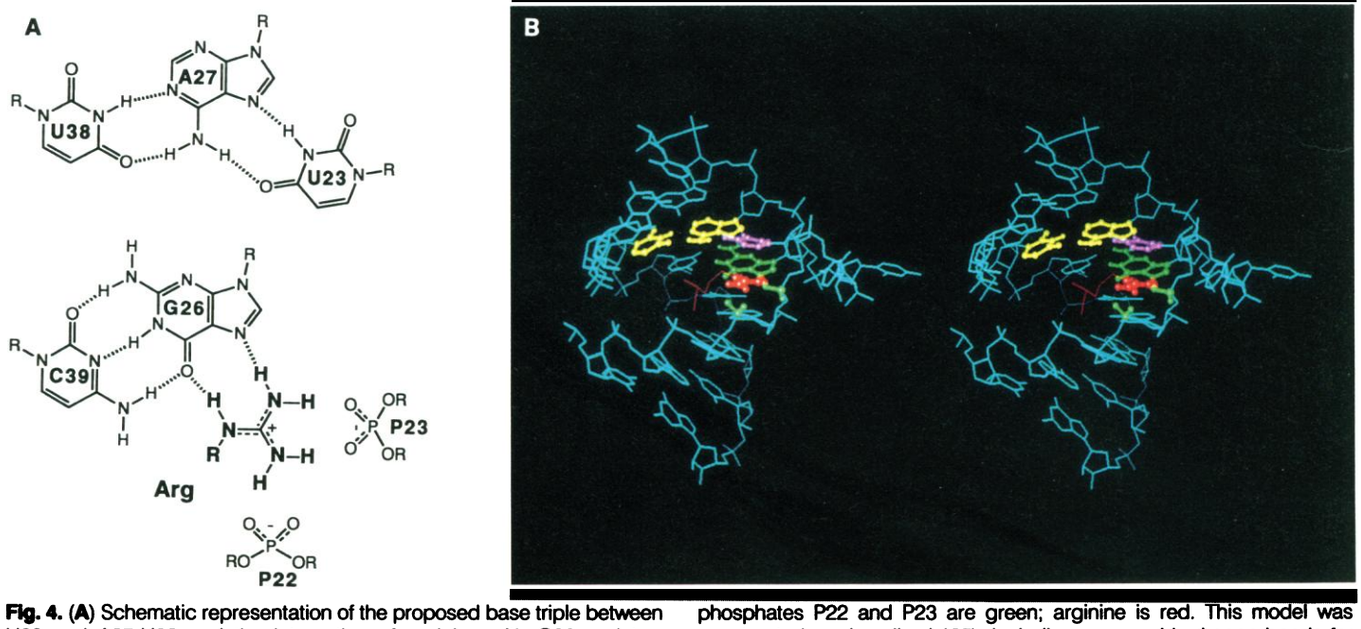

Fig. 4. (**A**) Schematic representation of the proposed base triple between U23 and A27·U38 and the interaction of arginine with G26 and two phosphate groups. (**B**) Stereo view of the model for the interaction of an arginine guanidinium group with TAR. The A27·U38 base pair is yellow, U23 is pink, and positions directly contacted by arginine, G26, and phosphates P22 and P23 are green; arginine is red. This model was constructed as described (*35*), including assumed hydrogen bonds for the arginine and base-triple interactions. Two hydrogen bond restraints were included between U23 and A27, two between arginine and G26, and one each to the nonbridging phosphate oxygens of P22 and P23.

The three-dimensional structure of TAR plays a critical role in specific arginine binding. Favorable binding energy is provided by hydrogen bonds to arginine as well as by the base-triple interaction. This favorable energy is partially offset by the energetic requirements of the RNA conformational change but can readily account for the 10- to 40-fold discrimination (1 to 2 kcal/mol) among TAR substrates (*8*). Specificity may be further improved by other interactions in the context of peptides or intact Tat protein.

The interaction of arginine with TAR highlights certain themes already observed in more complex RNA-protein interactions. Conformational changes involving unstacking of bases to make specific contacts have been observed in the two cocrystal structures of tRNAs with their cognate aminoacyl-tRNA synthetases (*1*, *2*). RNA-RNA interactions are important for stabilizing bound conformations in these complexes (*1*). Protein contacts often occur in single-stranded regions or at the junction of single- and double-stranded regions where bases are more accessible. Arginine may discriminate between base pairs in the major groove of TAR, and the presence of a bulge probably increases accessibility (*2*, *8*). Arginine makes many types of contacts with both bases and the phosphodiester backbone in crystal structures of DNA-protein (*31*) and RNA-protein complexes (*1*) and binds specifically to the guanosine binding site in the *Tetrahymena* intron (*32*). In a zinc finger domain–DNA crystal structure, an arginine interaction with guanine is stabilized by an additional interaction with a negatively charged aspartic acid (*27*), performed in TAR by an analogous interaction with phosphates. The interaction of arginine with TAR occurs in the absence of a protein structural context and emphasizes the importance of RNA structure in providing a specific binding site.

REFERENCES AND NOTES

1. M. A. Rould, J. J. Perona, D. Söll, T. A. Steitz, *Science* **246**, 1135 (1989); M. A. Rould, J. J. Perona, T. A. Steitz, *Nature* **352**, 213 (1991).
2. M. Ruff *et al.*, *Science* **252**, 1682 (1991).
3. B. Berkhout, R. H. Silverman, K.-T. Jeang, *Cell* **59**, 273 (1989); B. R. Cullen, *ibid.* **63**, 655 (1990); R. A. Marciniak, B. J. Calnan, A. D. Frankel, P. A. Sharp, *ibid.*, p. 791; A. D. Frankel, *Curr. Opin. Genet. Dev.* **2**, 293 (1992).
4. S. Roy, U. Delling, C.-H. Chen, C. A. Rosen, N. Sonenberg, *Genes Dev.* **4**, 1365 (1990).
5. C. Dingwall *et al.*, *EMBO J.* **9**, 4145 (1990).
6. B. J. Calnan, S. Biancalana, D. Hudson, A. D. Frankel, *Genes Dev.* **5**, 201 (1991).
7. B. Berkhout and K.-T. Jeang, *Nucleic Acids Res.* **19**, 6169 (1991).
8. K. M. Weeks and D. M. Crothers, *Cell* **66**, 577 (1991).
9. M. Sumner-Smith *et al.*, *J. Virol.* **65**, 5196 (1991); U. Delling *et al.*, *ibid.* **66**, 3018 (1992).
10. M. G. Cordingley *et al.*, *Proc. Natl. Acad. Sci. U.S.A.* **87**, 8985 (1990).
11. S. Feng and E. C. Holland, *Nature* **334**, 165 (1988).
12. B. J. Calnan, B. Tidor, S. Biancalana, D. Hudson, A. D. Frankel, *Science* **252**, 1167 (1991).
13. K. M. Weeks, C. Ampe, S. C. Schultz, T. A. Steitz, D. M. Crothers, *ibid.* **249**, 1281 (1990).
14. U. Delling *et al.*, *Proc. Natl. Acad. Sci. U.S.A.* **88**, 6234 (1991); T. Subramanian, R. Govindarajan, G. Chinnadurai, *EMBO J.* **10**, 2311 (1991).
15. J. Tao and A. D. Frankel, *Proc. Natl. Acad. Sci. U.S.A.* **89**, 2723 (1992).
16. G. Varani, C. Cheong, I. Tinoco, Jr., *Biochemistry* **30**, 3280 (1991); H. A. Heus and A. Pardi, *Science* **253**, 191 (1991); G. Varani and I. Tinoco, Jr., *Q. Rev. Biophys.* **24**, 479 (1991).
17. G. Varani, B. Wimberly, I. Tinoco, Jr., *Biochemistry* **28**, 7760 (1989); J. D. Puglisi, J. R. Wyatt, I. Tinoco, Jr., *J. Mol. Biol.* **214**, 437 (1990); *Biochemistry* **29**, 4215 (1990).
18. W. Saenger, *Principles of Nucleic Acid Structure* (Springer-Verlag, Berlin, 1984).
19. Milligram quantities of wild-type or mutant TAR RNAs (31 nucleotides) were synthesized with phage T7 RNA polymerase and purified as described (*6*, *33*). All of the NMR experiments were performed at RNA concentrations of 1.0 to 1.5 mM in 50 mM NaCl, 10 mM sodium phosphate (pH 6.5), and 0.1 mM sodium EDTA at 25°C unless otherwise indicated. Nonexchangeable proton NMR spectra were assigned by standard techniques including nuclear Overhauser exchange spectroscopy (NOESY) and double-quantum filtered–correlated and total correlation experiments (*16*, *17*, *34*). All aromatic (H6, H5, H8, and H2) and sugar proton (H1′, H2′, and H3′) resonances were assigned, and in some cases assignments were extended to H4′ and H5′/H5″. The NOESY spectra at mixing times between 50 and 200 ms were acquired for structure determination.
20. U23, C24, and U25 had majority populations of $C_{2'}$-*endo* conformations. The riboses of A22, G16, and C46 had heterogeneous ribose conformations, with large populations of $C_{2'}$-*endo*. Values of vicinal proton-to-proton coupling constants between ribose H1′ and H2′ protons were estimated from cross peaks in double-quantum filtered–correlated spectroscopy (COSY) experiments. Coupling constants between other ribose protons were determined from ^{31}P decoupled double-quantum filtered COSY experiments. Sugar conformations were estimated from coupling data [P. W. Davis, R. W. Adamiak, I. Tinoco, Jr., *Biopolymers* **29**, 109 (1990)].
21. F. A. Riordan, A. Bhattacharyya, S. McAteer, D. M. J. Lilley, *J. Mol. Biol.*, in press.
22. NMR experiments were performed with argininamide, the amide derivative of arginine. This analog, which lacks a negative charge of the arginine carboxyl group, binds to TAR with slightly higher affinity than does arginine (*15*).
23. Addition of 50 mM lysine caused no observable changes in the NMR spectrum of TAR, but high salt concentrations (>200 mM NaCl) inhibited argininamide binding. Chemical shift profiles for A22(H2) and G28(H8) as a function of argininamide concentration gave superimposable binding curves with a calculated dissociation constant of ~2 to 3 mM.
24. Argininamide is in fast exchange on the NMR time scale between bound and unbound forms (dissociation rate constants $>10^3$ s^{-1}). Intermolecular argininamide-TAR NOEs were negative, as were intramolecular TAR and intramolecular argininamide NOEs, as predicted for molecules or complexes with a relatively large (>1000) molecular weight (*34*).
25. R. Tan and A. D. Frankel, unpublished data.
26. Argininamide binds weakly to these mutants probably at sites different from the binding site in wt TAR. Weak NOEs were observed between argininamide and U25 in the C23 mutant and between argininamide and C45 in the U27·A38 mutant.
27. A base triple is formed by three hydrogen-bonded bases. Typically, the third nucleotide hydrogen bonds to a purine in the major groove edge of a Watson-Crick base pair. U-A·U triples have been observed in model systems (*18*).
28. NOEs were observed between the U23(H1′) proton and G26(H8) and G26(H3′) protons that constrain U23 in the region of A27. No exchangeable imino proton resonance from this base-triple interaction was observed, but this was not unexpected because the hydrogen bonds of this triple are exposed in the major groove and are expected to be highly accessible to solvent exchange.
29. N. P. Pavletich and C. O. Pabo, *Science* **252**, 809 (1991).
30. L. Chen and A. D. Frankel, unpublished data.
31. C. Wolberger, A. K. Vershon, B. Liu, A. D. Johnson, C. O. Pabo, *Cell* **67**, 517 (1991).
32. M. Yarus, *Science* **240**, 1751 (1988); M. Yarus, M. Illangesekare, E. Christian, *J. Mol. Biol.* **222**, 995 (1991).
33. J. F. Milligan and O. C. Uhlenbeck, *Methods Enzymol.* **180**, 51 (1989).
34. K. Wüthrich, *NMR of Proteins and Nucleic Acids* (Wiley, New York, 1986).
35. Models were developed with the NMRchitect (beta version) and Discover programs and displayed with Insight II (Biosym Technologies, San Diego, CA). Structures were generated by restrained molecular dynamics in a simulated annealing procedure with consistent valence force-field potentials in Discover. The upper and lower stems were restrained as A-form helices with dihedral restraints, and the loop region was not modeled. Ribose sugar conformations in the bulge were constrained as either C3′-*endo* or C2′-*endo* according to proton-to-proton coupling data. NOEs were characterized as strong, medium, or weak and given upper bounds of 2.5, 3.5, and 5.0 Å, respectively. In the unbound form, 17 NOE restraints were used in the bulge region, 7 weak, 5 medium, and 5 strong, of which 7 were intranucleotide restraints and 10 were internucleotide restraints. In the bound form, 13 NOE restraints were used in the bulge region, 5 weak, 7 medium, and 1 strong, of which 6 were intranucleotide and 7 were internucleotide contacts. In addition, in the bound form, 4 NOEs, 3 weak and 1 medium, were included to the δ proton of arginine, which was included as a single pseudoatom, and the glycosidic torsion for U23 was restrained in the range of 180° to 240°. Molecular dynamics were performed including only bond, angle, dihedral, and van der Waals energies. The annealing protocol began with an equilibration period at 10 K (10 ps), followed by rapid heating to 1000 K (3 ps), high-temperature dynamics (10 ps), and rapid cooling to 300 K (3 ps). Coulombic energies were then included for the final energy minimization. Three structures were generated for each form. The initial models for the unbound form were constructed with standard A-form helices, with a three-nucleotide gap opposite the bulge region. The starting point for the annealing of the bound form was the final unbound form. The root-mean-square (rms) deviation for the coordinates of the three unbound structures ranged from 3 to 9 Å, which is rather large as a result of variation of the orientation of the upper and lower helices. The rms deviation for the coordinates of the three bound structures ranged from 2.2 to 3.2 Å; these deviations are between 1.4 and 1.7 Å if the unstructured bulge nucleotides C24 and U25 are not included. Residual violations of the distance restraints for the structures shown were 0.21 and 0.26 Å for the unbound and bound forms, respectively.

36. We thank J. Tao for useful discussions and P. Davis, P. Kim, A. Pardi, L. Williams, and J. Wyatt for critical reading of the manuscript. Supported by a grant from the William M. Keck, Jr. Foundation, by the Lucille P. Markey Charitable Trust, by NIH grant AI29135 (A.D.F.), and by a grant from the Searle Scholars Program of The Chicago Community Trust (J.R.W.).

4 March 1992; accepted 8 May 1992